



Cite this: DOI: 10.1039/c6cc09095h

Received 14th November 2016,
Accepted 25th January 2017

DOI: 10.1039/c6cc09095h

rsc.li/chemcomm

Heterogeneous mesoporous manganese oxide catalyst for aerobic and additive-free oxidative aromatization of N-heterocycles†

Kankana Mullick, Sourav Biswas,‡ Alfredo M. Angeles-Boza* and Steven L. Suib*

Herein, we report a heterogeneous, aerobic, additive-free and environmentally benign catalytic protocol for oxidative aromatization of saturated nitrogen-heterocycles using a mesoporous manganese oxide material. The aromatized products can be separated by easy filtration and the catalyst is reusable for at least four cycles. Mechanistic investigation provides evidence for radical intermediates, a multi-electron redox cycle between Mn centers, and an oxygen exchange mechanism.

Nitrogen-containing heterocyclic aromatic compounds are common intermediates in pharmaceutical and biologically relevant molecules.^{1–4} The typical procedure to access heteroarenes involves dehydrogenation reactions from the corresponding saturated heterocycles. In the acceptorless dehydrogenation reaction, Fe-, Ru- and Ir-based catalysts have been used (Scheme 1A).^{5–10} More recently, metal-free boron based catalysts have been reported to catalyze this reaction.¹¹ An alternative procedure utilizes catalytic oxidative dehydrogenation of saturated nitrogen heterocycles under oxygen atmosphere (Scheme 1B). Several homogeneous catalysts have been successfully employed for the oxidative dehydrogenation route.^{12–16} From an environmental perspective, heterogeneous catalysts are preferred due to the facile product separation and the prospects of catalyst reusability. Some existing heterogeneous catalysts for oxidative aromatization of N-heterocycles are Rh-, Pd-, and Pt-based catalysts, Pd₃Pb, Au nanoparticles, and Ru supported on different metal oxide supports.^{17–24} Notably, most of the systems are based on less abundant precious metals and display narrow substrate scope.

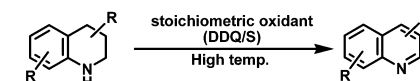
Beller and co-workers have reported an efficient heterogeneous iron–nitrogen doped graphene core–shell catalyst with

A. Acceptorless dehydrogenation

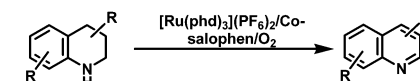


B. Oxidative dehydrogenation

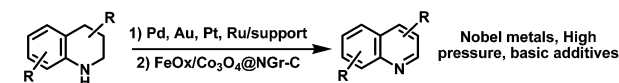
Traditional



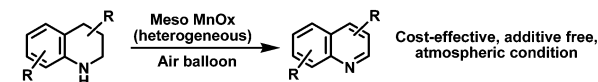
Homogeneous



Heterogeneous



This Work



Scheme 1 Various routes to synthesize N-heterocyclic aromatic compounds.

broad substrate scope and excellent reusability.²⁵ Additionally, Stahl and co-workers have used cobalt oxide supported nitrogen doped graphene catalysts for oxidative aromatization at low temperatures.²⁶ Despite their good catalytic performance, these systems require either difficult catalyst preparation methods or use of high oxygen pressure and additives. Therefore, a simple, efficient heterogeneous catalytic system for oxidative aromatization of N-heterocycles under aerobic, atmospheric conditions is highly desirable.

We have designed a series of mesoporous materials by an inverse-micelle templated evaporation induced self-assembly technique.²⁷ Mesoporous manganese oxide materials prepared by this method showed excellent performance in aerobic oxidation of alcohols to aldehydes, amines to imines, anilines to azo compounds, tandem oxidative reactions from alcohols, and

Department of Chemistry, University of Connecticut, 55 North Eagleville Rd., Storrs, Connecticut 06269, USA. E-mail: alfredo.angeles-boza@uconn.edu, steven.suib@uconn.edu

† Electronic supplementary information (ESI) available: Experimental details, Tables S1–S4, Fig. S1–S12 and Schemes S1–S3 and spectral characterization of typical products. See DOI: 10.1039/c6cc09095h

‡ Present address: Department of Chemistry, University of Wisconsin-Madison, 1101 University Avenue, Madison, Wisconsin 53706, USA.

oxidative coupling of alkynes to diyne derivatives.^{28–32} These manganese oxide materials have versatile structural forms with high thermal stability. The manganese redox cycling and labile lattice oxygen molecules have been shown to be determinant factors in the catalytic performance of these novel materials. Herein, we present our effort to use mesoporous manganese oxide materials for the aerobic dehydrogenation of saturated N-heterocycles to their corresponding aromatic derivatives. Absence of precious metals and additives, use of air as the sole oxidant, easy isolation of products, along with proper catalyst reusability make our catalytic protocol an attractive choice for oxidative aromatization of N-heterocyclic compounds.

To examine the activity of the manganese oxide catalysts we initially selected 1,2,3,4-tetrahydroquinoline as the test substrate. In a comparative study, 1,2,3,4-tetrahydroquinoline was reacted with different phases of well-known manganese oxide materials for oxidation reactions. The mesoporous manganese oxide material (meso MnOx), prepared by an inverse micelle templated self-assembly method,²⁷ provided a 50% conversion with >99% selectivity to the target compound quinoline in aerobic conditions (Table 1, entry 1). No improvement of activity was observed by introducing Cs promoter ions (Table 1, entry 2). Relatively higher conversions were achieved using two other active manganese oxide phases, octahedral molecular sieves (K-OMS-2) and amorphous manganese oxide (AMO),³³ however selectivity decreased significantly due to formation of N-oxide by over oxidation (Table 1, entries 3 and 4). Notably, a reaction with commercial nonporous Mn₂O₃ gave negligible conversion, similar to catalyst-free conditions (Table 1, entries 5 and 6). The continual increase of performance with catalyst loading (Table 1, entries 7–9) indicates that the system is not suffering from adsorption and mass transfer. The reaction was also surveyed with different solvents of varying polarity. As revealed in Table S1 (ESI[†]), the reaction was facilitated in the presence of polar solvents and *N,N*-dimethylformamide (DMF) emerged as the best solvent.

The mesoporous manganese oxide materials were synthesized by an inverse micelle templated method, where a non-polar

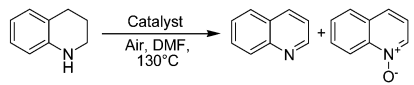
pluronic surfactant (P123) was used as the building block. The material was formed by aggregation of nanoparticles with intraparticle voids within the mesostructure. As indicated by the powder X-ray diffraction measurements (Fig. S1, ESI[†]) the material was amorphous at low calcination temperatures (<350 °C) and formed a crystalline bixbyite (Mn₂O₃) phase at higher temperatures (>400 °C). The mesoporous structure of meso MnOx was confirmed by nitrogen sorption studies (Fig. S2a, ESI[†]), where a type IV adsorption isotherms, followed by type I hysteresis loop were observed irrespective of calcination temperatures. The material possessed uniform mesoporous size distributions (Fig. S2b, ESI[†]) and an increment in pore size was observed with higher calcination temperature due to sintering of the nanoparticles (Table S2, ESI[†]). The oxidation states of Mn (determined by X-ray photoelectron spectra [XPS]) was found to be 3+ at different calcination temperatures (Fig. S3, ESI[†]). The O 1s XPS (Fig. S4, ESI[†]) of meso MnOx-250 showed features typical of manganese oxide materials having multiple oxygen species.

The high surface area and poor crystalline nature of the material are critical for achieving high efficiency. Highly accessible surface area provides larger amounts of catalytically active sites, whereas the poor crystalline nature of the material results in highly accessible and labile lattice oxygen. The performance of the meso MnOx material was investigated as a function of calcination temperatures, since calcination has a remarkable effect on the surface area and crystallinity of the material (Fig. S5, ESI[†]). The highest conversion (72%) was achieved when the material was calcined to 350 °C (highest surface area, 226 m² g⁻¹ and amorphous in nature) and the conversion decreased significantly when the material was heated to 450 °C (26%) due to lowering of surface area (150 m² g⁻¹) and increasing crystallinity.

While investigating the role of oxidant, the reaction under pure molecular oxygen instead of air did not improve the conversion but reduced the selectivity of quinoline due to over-oxidation (Table S3, entries 1 and 2, ESI[†]). However, conversion was increased significantly under a pressurized oxygen system using lower amounts of catalyst (Table S3, entries 3 and 4, ESI[†]). This is due to the higher solubility of oxygen in the solvent under high pressure. Therefore, after extensive screening of all reaction parameters, we chose aerobic conditions in DMF at 130 °C as the optimal reaction condition for the meso MnOx-350 catalyst.

Preventing deactivation of catalysts due to aggregation and leaching of active metals in solution is a challenge for heterogeneous catalytic systems. To verify for leaching of active metals, we performed a hot filtration (Fig. S6, ESI[†]). The catalyst was removed from the reaction system after 3 h (at about 30% conversion) and the filtrate was kept under the same reaction conditions for the next 20 h. No further reaction was observed, which confirmed the absence of active metals in the solution. To check for reusability, the catalyst was retrieved from the reaction mixture by centrifugation and washed with excess DMF and ethanol. Prior to reuse, the catalyst was reactivated at 250 °C for 30 min to remove any adsorbed substrates. As observed in Fig. S7a (ESI[†]) the catalyst can be reused for at least four times without any loss of activity and selectivity.

Table 1 Comparison of catalysts for aromatization of 1,2,3,4-tetrahydroquinoline^a



Entry	Catalyst	Catalyst amount (mg)	Conv. ^b (%)	Selec. ^b (%)
1	Meso MnOx	25	50	> 99
2	Meso Cs/MnOx	25	50	> 99
3	K-OMS-2	25	65	70
4	AMO	25	60	90
5	C-Mn ₂ O ₃	25	1	> 99
6	No	0	1	> 99
7	Meso MnOx	5	11	> 99
8	Meso MnOx	10	25	> 99
9	Meso MnOx	50	80	> 99

^a Reaction conditions: 1,2,3,4-tetrahydroquinoline (0.25 mmol), catalyst (required amount), DMF (5 mL), 130 °C, air balloon, 5 h. ^b Conversions and selectivity were determined by GC-MS based on concentration of 1,2,3,4-tetrahydroquinoline.

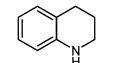
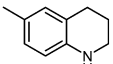
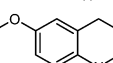
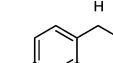
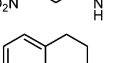
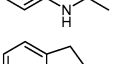
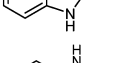
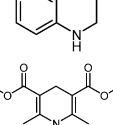
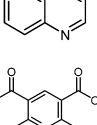
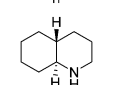
Additionally, the X-ray diffraction studies confirmed that the amorphous nature of the catalyst was retained after multiple reuse cycles (Fig. S7b, ESI†). Therefore, our catalyst is heterogeneous, stable, and reusable.

The kinetic aspects of the reaction were determined by conducting a time-dependent study (Fig. S8, ESI†). Formation of quinoline *N*-oxide was observed in trace amounts after 3 h. A first order rate equation was derived with respect to 1,2,3,4-tetrahydroquinoline with a rate constant of $(2.9 \pm 0.1) \times 10^{-5} \text{ s}^{-1}$ (Fig. S9, ESI†). A series of time-dependent experiments were performed in the temperature range of 80–140 °C. The apparent activation energy was estimated as $8.3 \pm 0.2 \text{ kcal mol}^{-1}$ using the Arrhenius equation (Fig. S10, ESI†).

The current methodology works well for a diverse library of N-containing aromatic heterocycles. The products can be isolated easily by filtration followed by solvent evaporation. Isolated yields of some of the aromatized products along with their NMR spectra are provided (see ESI†). The presence of electron donating substituents in the aromatic ring of 1,2,3,4-tetrahydroquinoline did not alter the catalytic activity (entries 2 and 3, Table 2). The present protocol can be applicable to functional groups containing electron lone pairs (–OMe), which were found to partially deactivate the aforementioned boron-based catalytic system due to coordination.¹¹ The presence of the electron withdrawing group –NO₂ in the aromatic ring resulted in moderate conversions (70%, entry 5, Table 2). These results can be interpreted as a measure of the susceptibility of the catalytic efficiency to substituent effects. Substitutions at position 2 of the saturated ring of 1,2,3,4-tetrahydroquinoline resulted in lower conversion due to steric effects that retard the abstraction of the α C–H hydrogen (entry 5, Table 2). Quinoxaline and indole derivatives are representative structural motifs in biologically and pharmaceutically relevant molecules.³⁴ The oxidative dehydrogenation method by meso MnOx could be an attractive synthetic route for preparation of quinoxaline and indole. As observed, a substituted 2-methylindoline and a saturated 1,2,3,4-tetrahydroquinoxaline can be effectively aromatized with quantitative conversion (>99%) and selectivity (entries 6 and 7, Table 2). The excellent functional group tolerance of the present protocol was exhibited by the oxidative aromatization of Hantzsch ester, which yielded the desired aromatic product with quantitative conversion (>99%) and excellent selectivity (>99%) at lower temperature and short reaction time (entry 8, Table 2). On the other hand, N heterocycles lacking an adjacent ancillary benzene ring did not produce any product (entry 9, Table 2).

Several control experiments were then performed to gain mechanistic insights of the present catalytic protocol. In the report by Beller and co-workers, the reaction is initiated by forming a radical intermediate by transfer of electron from 1,2,3,4-tetrahydroquinoline to the catalyst. By introducing the radical scavenger 2,6-di-*tert*-butyl-4-methylphenol in the reaction mixture, we trapped the radical intermediate formed after the electron transfer step (Scheme S1, ESI†). This result suggested similar reaction pathways for our system and the catalyst reported by Beller and co-workers.²⁵ A reaction of 1,2,3,4-tetrahydronaphthalene only produced the oxidized

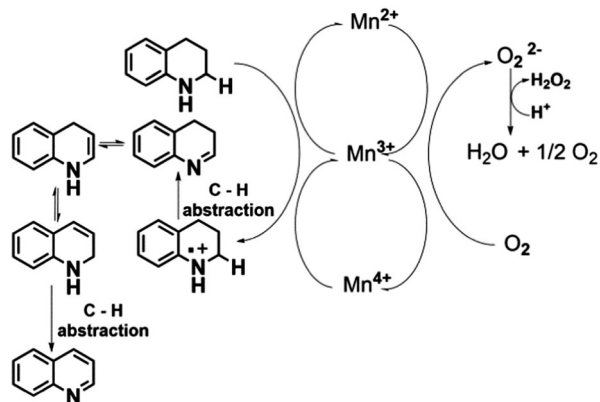
Table 2 Oxidative dehydrogenation of N-heterocycles by meso MnOx^a

No.	Substrate	Product	Conv. ^b (%)	Sel. ^b (%)	TON ^c
1			>99	95	1.7
2			>99	>99	1.7
3			>99	93 (89)	1.7
4			70	>99	1.4
5			80	>99	1.5
6			>99	>99	1.7
7			>99	>99 (92)	1.7
8 ^d			>99	>99 (94)	1.7
9		nd	0	0	0

^a Reaction conditions: substrate (0.25 mmol), meso MnOx (25 mg), DMF (3 mL), 130 °C, 20 h, air balloon. ^b Conversion and selectivity were determined by GC-MS. Numbers in parenthesis refer to yields of isolated products. Isolation was carried out in acetonitrile at 80 °C. ^c TON = moles of amines converted/moles of catalyst. ^d 120 °C and 5 h. nd = not determined.

products (corresponding alcohol and ketone) with negligible conversion (Scheme S2, ESI†) indicating that direct C–C dehydrogenation is unlikely to occur in the present reaction conditions. Therefore, the presence of nitrogen in the saturated cyclic alkane moiety is necessary to begin the reaction by transferring an electron to the Mn center. The formed amine radical species can then undergo α C–H dehydrogenation to form an imine (C=N) intermediate (Scheme 2). This is reinforced by the fact that, substrate lacking an α C–H proton (1,2,3,4-tetrahydro-2,2,4,7-tetramethylquinoline, Scheme S3, ESI†) did not form any product. The final aromatized product is probably formed by a second dehydrogenation from a tautomeric cyclic imine as reported by Jones and co-workers.⁵

The formation of the radical amine intermediate results in the reduction of surface active Mn centers, which leads to release of labile lattice oxygen.^{29,32} Under catalytic turnover conditions, the reduced Mn species can be re-oxidized by dioxygen with production of H₂O₂, which can disproportionate to water and O₂ in the presence of manganese oxide.³⁵ The aerobic atmosphere is critical as loss of lattice oxygen should be replenished by the aerial oxygen. This is consistent with the observation of lower catalytic efficiency under nitrogen atmosphere (18% conversion) compared to aerobic conditions (50% conversion).



Scheme 2 Proposed mechanism of oxidative aromatization of 1,2,3,4-tetrahydroquinoline.

A kinetic analysis under nitrogen atmosphere revealed a decrease of conversion after 4 h, which may be due to incomplete re-oxidation of reduced Mn species due to lack of oxygen (Fig. S11, ESI[†]). Additionally, we characterized the material by XPS after reaction under nitrogen atmosphere (Fig. S12, ESI[†]). The significant decrease (22.8%) in lattice oxygen (O_s) compared to the bare material (62.6%) indicates the presence of oxygen vacancies due to incomplete replenishment under nitrogen atmosphere (Table S4, ESI[†]). The Mn 2p spectrum of the material used under N_2 atmosphere shows a mixture of Mn valency (a higher Mn oxidation state at 642.5 eV and a lower Mn oxidation state at 639.4 eV)³⁶ indicative of incomplete re-oxidation. These results allowed us to suggest a mechanism consistent with multielectron transfer between the Mn centers and the substrate with the involvement of labile lattice oxygen in the catalytic cycle (Scheme 2).

In summary, we presented a heterogeneous, cost-effective, and mild reaction procedure for oxidative aromatization of diverse nitrogen heterocycles with readily abundant manganese oxide materials. The use of air as the terminal oxidant, absence of precious metals and ligand additives, along with catalyst reusability and easy isolation of the aromatized products make our catalytic protocol green and environmentally benign. The mechanistic studies invoked a Mn-mediated radical species formation, followed by two successive dehydrogenation steps. Although optimal conditions required high temperature (130 °C) and DMF as solvent, the reaction also worked at a lower temperature (80 °C) in acetonitrile with formation of desired product in >95% yield when larger catalyst loadings were used. High surface area, the amorphous nature, and the involvement of labile lattice oxygen are important factors for the catalytic efficiency of meso MnOx.

AMAB acknowledges the financial support from the University of Connecticut. SLS thanks support of the US Department of Energy, Office of Basic Energy Sciences, Division of Chemical, Biological and Geological Sciences under grant DE-FG02-86ER13622.A000.

Notes and references

- 1 A. Deiters and S. F. Martin, *Chem. Rev.*, 2004, **104**, 2199–2238.
- 2 E. Vitaku, D. T. Smith and J. T. Njardarson, *J. Med. Chem.*, 2014, **57**, 10257–10274.
- 3 S. Süzen, *Bioactive Heterocycles V*, Springer, 2007, pp. 145–178.
- 4 B. Zhang and A. Studer, *Chem. Soc. Rev.*, 2015, **44**, 3505–3521.
- 5 S. Chakraborty, W. W. Brennessel and W. D. Jones, *J. Am. Chem. Soc.*, 2014, **136**, 8564–8567.
- 6 K.-i. Fujita, Y. Tanaka, M. Kobayashi and R. Yamaguchi, *J. Am. Chem. Soc.*, 2014, **136**, 4829–4832.
- 7 J. Wu, D. Talwar, S. Johnston, M. Yan and J. Xiao, *Angew. Chem.*, 2013, **125**, 7121–7125.
- 8 W. Yao, Y. Zhang, X. Jia and Z. Huang, *Angew. Chem., Int. Ed.*, 2014, **53**, 1390–1394.
- 9 R. Yamaguchi, C. Ikeda, Y. Takahashi and K.-i. Fujita, *J. Am. Chem. Soc.*, 2009, **131**, 8410–8412.
- 10 D. Talwar, A. Gonzalez-de-Castro, H. Y. Li and J. Xiao, *Angew. Chem., Int. Ed.*, 2015, **54**, 5223–5227.
- 11 M. Kojima and M. Kanai, *Angew. Chem.*, 2016, **128**, 12412–12415.
- 12 A. E. Wendlandt and S. S. Stahl, *Org. Lett.*, 2012, **14**, 2850–2853.
- 13 A. E. Wendlandt and S. S. Stahl, *J. Am. Chem. Soc.*, 2013, **136**, 506–512.
- 14 A. E. Wendlandt and S. S. Stahl, *J. Am. Chem. Soc.*, 2014, **136**, 11910–11913.
- 15 A. E. Wendlandt and S. S. Stahl, *Angew. Chem., Int. Ed.*, 2015, **54**, 14638–14658.
- 16 D. L. Evans, D. K. Minster, U. Jordis, S. M. Hecht, A. L. Mazzu Jr and A. Meyers, *J. Org. Chem.*, 1979, **44**, 497–501.
- 17 K. Yamaguchi and N. Mizuno, *Angew. Chem., Int. Ed.*, 2003, **42**, 148–1483.
- 18 D. Damodara, R. Arundhathi and P. R. Likhar, *Adv. Synth. Catal.*, 2014, **356**, 189–198.
- 19 M. Amende, C. Gleichweit, K. Werner, S. Schernich, W. Zhao, M. P. Lorenz, O. Höfert, C. Papp, M. Koch and P. Wasserscheid, *ACS Catal.*, 2014, **4**, 657–665.
- 20 S. Furukawa, A. Suga and T. Komatsu, *Chem. Commun.*, 2014, **50**, 3277–3280.
- 21 M. H. So, Y. Liu, C. M. Ho and C. M. Che, *Chem. – Asian J.*, 2009, **4**, 1551–1561.
- 22 H. Yuan, W.-J. Yoo, H. Miyamura and S. Kobayashi, *J. Am. Chem. Soc.*, 2012, **134**, 13970–13973.
- 23 D. V. Jawale, E. Gravel, N. Shah, V. Dauvois, H. Li, I. N. Namboothiri and E. Doris, *Chem. – Eur. J.*, 2015, **21**, 7039–7042.
- 24 D. Ge, L. Hu, J. Wang, X. Li, F. Qi, J. Lu, X. Cao and H. Gu, *ChemCatChem*, 2013, **5**, 2183–2186.
- 25 X. Cui, Y. Li, S. Bachmann, M. Scalone, A.-E. Surkus, K. Junge, C. Topf and M. Beller, *J. Am. Chem. Soc.*, 2015, **137**, 10652–10658.
- 26 A. V. Iosub and S. S. Stahl, *Org. Lett.*, 2015, **17**, 4404–4407.
- 27 A. S. Poyraz, C.-H. Kuo, S. Biswas, C. K. King'onde and S. L. Suib, *Nat. Commun.*, 2013, **4**, 2952.
- 28 S. Biswas, A. S. Poyraz, Y. Meng, C.-H. Kuo, C. Guild, H. Tripp and S. L. Suib, *Appl. Catal., B*, 2015, **165**, 731–741.
- 29 S. Biswas, B. Dutta, K. Mullick, C.-H. Kuo, A. S. Poyraz and S. L. Suib, *ACS Catal.*, 2015, **5**, 4394–4403.
- 30 S. Biswas, K. Mullick, S.-Y. Chen, A. Guduz, D. M. Carr, C. Mendoza, A. M. Angeles-Boza and S. L. Suib, *Appl. Catal., B*, 2017, **203**, 607–614.
- 31 S. Biswas, K. Mullick, S.-Y. Chen, D. A. Kriz, M. Shakil, C.-H. Kuo, A. M. Angeles-Boza, A. R. Rossi and S. L. Suib, *ACS Catal.*, 2016, **6**, 5069–5080.
- 32 B. Dutta, S. Biswas, V. Sharma, N. O. Savage, S. Alpay and S. L. Suib, *Angew. Chem.*, 2016, **128**, 2211–2215.
- 33 S. L. Suib, *Acc. Chem. Res.*, 2008, **41**, 479–487.
- 34 L. E. Seitz, W. J. Suling and R. C. Reynolds, *J. Med. Chem.*, 2002, **45**, 5604–5606.
- 35 V. D. Makwana, Y.-C. Son, A. R. Howell and S. L. Suib, *J. Catal.*, 2002, **210**, 46–52.
- 36 H. C. Genuino, S. Dharmarathna, E. C. Njagi, M. C. Mei and S. L. Suib, *J. Phys. Chem. C*, 2012, **116**, 12066–12078.